

Surface effects on the isovector spin response induced by high energy protons

H. Esbensen,* H. Toki,† and G. F. Bertsch*

Cyclotron Laboratory and Department of Physics-Astronomy,
Michigan State University, East Lansing, Michigan 48824

(Received 18 October 1984)

The isovector longitudinal and the transverse spin responses of heavy nuclei, induced by high energy proton scattering, are studied using the surface response technique. The large enhancement of the longitudinal over the transverse spin response obtained in infinite nuclear matter is found to be weakened in the surface response model. The remaining discrepancy from recent proton scattering data can essentially be explained by the isoscalar background.

I. INTRODUCTION

Recently, Carey *et al.*¹ have measured a complete set of polarization-transfer observables at the momentum transfer of $q = 1.75 \text{ fm}^{-1}$ using 500 MeV protons scattered inelastically from ^2H and ^{208}Pb at Los Alamos Meson Physics Facility (LAMPF). The derived longitudinal and transverse responses show no difference between the two responses, even in Pb. This result seems to show a failure of the model of the spin-isospin interactions based on the pion and rho-meson exchanges, which has been used to describe a wide variety of pionic and spin-dependent phenomena (see Ref. 2 and references quoted therein). The model interaction is attractive in the longitudinal channel and repulsive in the transverse channel at $q = 1.75 \text{ fm}^{-1}$, and the responses in these two channels are therefore expected to be different, as indicated by infinite nuclear matter calculations.³

This model has also been used as the basis for a plausible explanation⁴⁻⁷ of the so-called European Muon Collaboration (EMC) effect⁸ in which the quark structure function, probed by inelastic muon scattering, shows an enhancement in heavy nuclei. In particular, the model interaction results in an enhancement of the pionic field in the momentum range $q \sim 1.5-2 \text{ fm}^{-1}$ due to the nuclear medium, which increases the structure function in the appropriate kinematic region. Hence, the experimental fact that the longitudinal response is not enhanced compared to the transverse response in the proton experiment seems to provide an argument against the pionic interpretation of the EMC effect.

The response of heavy nuclei to high energy proton scattering, however, depends strongly on the surface region of the nucleus. Bertsch and Scholten⁹ have developed a technique, based on the Glauber theory,^{10,11} to treat the surface response for quasielastic scattering. For (p, p') reactions they find that the largest contribution to the response comes from the tail of the density distribution, in the vicinity of one-half or one-quarter of nuclear matter density, the precise position depending on the size of the nucleus and the incoming proton energy. Thus the calculated response differs significantly from that of infinite nuclear matter. This technique has been extended¹² to include the effect of residual interactions using the

self-consistent linear response theory, or random-phase approximation (RPA); and the model predictions agree quite well with measured quasielastic (p, p') cross sections at 319 and 800 MeV.

Therefore, it remains to be seen how the surface response to the longitudinal field $\sigma \cdot \mathbf{q} e^{i(\mathbf{q} \cdot \mathbf{r} - \omega t)}$ and to the transverse field $\sigma \times \mathbf{q} e^{i(\mathbf{q} \cdot \mathbf{r} - \omega t)}$ behaves when we use the same model as is used to describe the pionic data.

Before going into details, it is important to recognize that the EMC effect is caused by the nucleus as a whole (volume effect) as the leptons penetrate through the nucleus, while the spin response in high energy nucleon scattering is induced at the nuclear surface. Hence, to compare these two kinds of observables, a careful study of surface effects is needed.

II. FORMALISM

We shall follow the model of the surface response of Fermi liquids, where a semi-infinite slab geometry is assumed.¹² Hence, we will not repeat all the details of the formalism and ask readers to see Ref. 12. We only provide here the isovector spin-isospin interactions, which transmit the longitudinal as well as the transverse response through the nuclear medium.

The spin-isospin interactions written for particle-hole matrix elements are given by (in momentum space)

$$\begin{aligned}
 W_{\text{ph}} = & \frac{f_{\pi}^2}{m_{\pi}^2} \Gamma_{\pi}^2 \frac{\sigma_1 \cdot \mathbf{q} \sigma_2 \cdot \mathbf{q}}{\omega^2 - q^2 - m_{\pi}^2} \tau_1 \cdot \tau_2 \\
 & + \frac{f_{\rho}^2}{m_{\rho}^2} \Gamma_{\rho}^2 \frac{\sigma_1 \times \mathbf{q} \cdot \sigma_2 \times \mathbf{q}}{\omega^2 - q^2 - m_{\rho}^2} \tau_1 \cdot \tau_2 \\
 & + \frac{f_{\pi}^2}{m_{\pi}^2} \Gamma_{\pi}^2 g' \sigma_1 \cdot \sigma_2 \tau_1 \cdot \tau_2
 \end{aligned} \tag{1}$$

with the standard notations.² In addition to the one pion exchange (first term) and the rho-meson exchange (second term), the third term is added to take into account the short range correlations and the exchange contributions. The phenomenological parameter g' (so-called Landau parameter) seems to be around $g' \sim 0.6$ through the study of low-lying unnatural parity states.^{13,14} This value includes the effect of polarizations in the delta-hole excitation

channel. Since we treat this channel explicitly in our numerical calculations, the appropriate value of g' is slightly larger, and we shall use $g'=0.7$. The preceding interaction also applies in the delta-hole excitation channel, except for the fact that the strengths are larger: $f_{\pi\Delta h}^*=2f_{\pi ph}$ and $f_{\rho\Delta h}^*=2f_{\rho ph}$.

Using the identity

$$\sigma_1 \cdot \sigma_2 = \sigma_1 \cdot \hat{\mathbf{q}} \sigma_2 \cdot \hat{\mathbf{q}} + \sigma_1 \times \hat{\mathbf{q}} \cdot \sigma_2 \times \hat{\mathbf{q}}, \quad (2)$$

the spin-isospin interaction is separated into the longitudinal W_{ph}^L and the transverse W_{ph}^T parts:

$$W_{ph} = [W_{ph}^L(\mathbf{q})\sigma_1 \cdot \hat{\mathbf{q}}\sigma_2 \cdot \hat{\mathbf{q}} + W_{ph}^T(\mathbf{q})\sigma_1 \times \hat{\mathbf{q}} \cdot \sigma_2 \times \hat{\mathbf{q}}]\tau_1 \cdot \tau_2, \quad (3)$$

where

$$W_{ph}^L(\mathbf{q}) = \frac{f_\pi^2}{m_\pi^2} \Gamma_\pi^2 \left[g' - \frac{q^2}{q^2 + m_\pi^2 - \omega^2} \right], \quad (4a)$$

and

$$W_{ph}^T(\mathbf{q}) = \frac{f_\pi^2}{m_\pi^2} \left[g' \Gamma_\pi^2 - C_\rho \Gamma_\rho^2 \frac{q^2}{q^2 + m_\rho^2 - \omega^2} \right], \quad (4b)$$

with

$$C_\rho = f_\rho^2 m_\pi^2 / (f_\pi^2 m_\rho^2) \simeq 2.18.$$

The momentum dependence of the longitudinal and the transverse interactions for a standard set of parameters³ is shown in Fig. 1. In the longitudinal channel, the pionic attraction wins against the short range repulsion in the momentum range of $q > 1 \text{ fm}^{-1}$ due to the small mass of the pion, while in the transverse channel, the interaction stays positive even at reasonably large momentum transfers. Hence, the response functions in the two channels at large q , $q \sim 2 \text{ fm}^{-1}$, should behave differently through the preceding spin-isospin correlations. The question is now how large are the nuclear medium effects on the independent particle response in the two channels.

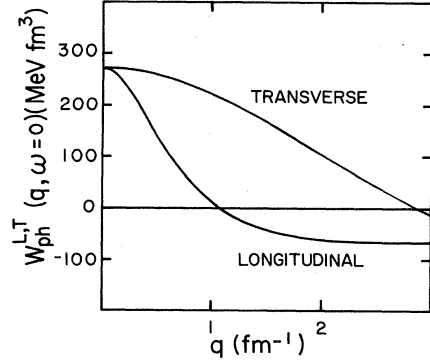


FIG. 1. Momentum dependence of the longitudinal and the transverse interactions [Eqs. (4a) and (4b)]. The parameters used are the same as those used in Ref. 3, i.e., $f_\pi=1$, $C_\rho=2.18$, $\Lambda_\pi=1.3 \text{ GeV}$, $\Lambda_\rho=2 \text{ GeV}$, and $g'=0.7$.

In finite nuclei, the two channels are not orthogonal due to the fact that the momentum is not a good quantum number. However, Toki and Weise¹⁵ have shown in explicit computations that these two channels do not interfere even for nuclei as small as ^{12}C , using reasonable interaction strengths. Hence, we shall treat the interactions independently and use W_{ph}^L for the longitudinal response and W_{ph}^T for the transverse response.

A. Slab geometry

It is convenient to express the interactions in coordinate space for the surface direction (z direction), while the momentum space representation, $\mathbf{q}_{\parallel}=\mathbf{K}$, is kept in the x - y direction;¹²

$$W_{ph}^{L,T}(K, z-z') = \int \frac{dq_z}{2\pi} W_{ph}^{L,T}(K, q_z) e^{iq_z(z-z')}. \quad (5)$$

In this representation the longitudinal interaction is given by

$$W_{ph}^L(K, z-z') = \frac{f_\pi^2}{m_\pi^2} \Gamma_\pi^2 \left[(g'-1)\delta(z-z') + \frac{m_\pi^2 - \omega^2}{K^2 + m_\pi^2 - \omega^2} \frac{1}{2a_\pi} \exp\left(-\frac{|z-z'|}{a_\pi}\right) \right], \quad (6)$$

where the finite range is $a_\pi = 1/(K^2 + m_\pi^2 - \omega^2)^{1/2}$. The transverse interaction can be written in a similar way

$$W_{ph}^T(K, z-z') = \frac{f_\pi^2}{m_\pi^2} \left[(g' \Gamma_\pi^2 - C_\rho \Gamma_\rho^2) \delta(z-z') + C_\rho \Gamma_\rho^2 \frac{m_\rho^2 - \omega^2}{K^2 + m_\rho^2 - \omega^2} \frac{1}{2a_\rho} \exp\left(-\frac{|z-z'|}{a_\rho}\right) \right], \quad (7)$$

with the finite range $a_\rho = 1/(K^2 + m_\rho^2 - \omega^2)^{1/2}$. The finite range for this interaction is much smaller ($a_\rho \sim 0.25 \text{ fm}$) than for the longitudinal field ($a_\pi \sim 1.4 \text{ fm}$), due to the much larger mass of the rho meson.

The field-free polarization propagator for particle-hole excitations $\Pi_{ph}^0(z, z', K, \omega)$ is calculated for slab geometry as described in Ref. 12, and it is identical to minus the field-free Green's function used there. In defining the particle-hole and delta-hole polarization propagators, we

include the spin-isospin factors of 4 and $\frac{16}{9}$ in the definition of these operators, respectively. Moreover, the larger strength of the Δ vertex, $f_{\pi\Delta h}^*=2 \cdot f_{\pi ph}$, is included as a factor of 4 in the polarization operator $\Pi_{\Delta h}^0$ for delta-hole excitations, so that the total polarization operator is

$$\Pi^0 = \Pi_{ph}^0 + \Pi_{\Delta h}^0, \quad (8)$$

and the associated RPA polarization operator for the longitudinal and the transverse response becomes

$$\Pi_{\text{RPA}}^{L,T} = (1 - \Pi^0 W_{\text{ph}}^{L,T})^{-1} \Pi^0. \quad (9)$$

The inverse operator in this equation is calculated by numerical inversion of its matrix representation on a finite grid in the two z coordinates.

B. External field

The inelastic cross sections for proton scattering, calculated in Refs. 9 and 12, were obtained as a product of the free nucleon-nucleon cross section, the surface response of a semi-infinite slab of nuclear matter, and a normalization factor. The latter two quantities were determined consistently with the Glauber theory for single scattering on a finite nucleus. We shall apply the same method to determine the surface response, and we shall therefore remind the reader of the procedure.

The external field $V_{\text{ext}}(z)$ used to generate the surface response

$$S(\mathbf{q}, \omega) = -\frac{1}{\pi} \text{Im} \int dz dz' V_{\text{ext}}^*(z) \Pi(z, z', q_{\parallel}, \omega) V_{\text{ext}}(z') \quad (10)$$

contains a plane wave associated with the z component (perpendicular to the surface of the slab) of the momentum transfer \mathbf{q} to the incoming proton. The component along the surface, q_{\parallel} , is already built into the polarization operator. It has the form

$$V_{\text{ext}}(z) = F(z) \exp(iq_z z). \quad (11)$$

The function $F(z)$ contains the effect of absorption in the single-scattering channel, and it is determined by

$$\begin{aligned} |F(z)|^2 \rho_0(z) &= \frac{d\sigma^{(1)}}{dz} \\ &= 2\pi(R+z)\chi(z)\exp[-\chi(z)]. \end{aligned} \quad (12)$$

Here $\rho_0(z)$ is the nuclear density of the slab. The right-hand side is the (differential) contribution to the cross section for single scattering on a finite nucleus of radius R , and

$$\chi(z) = \int dx \rho_{\text{FN}} \{r = [x^2 + (R+z)^2]^{1/2}\} \sigma_{\text{NN}} \quad (13)$$

is the average number of collisions, σ_{NN} being the total nucleon-nucleon cross section, and $\rho_{\text{FN}}(r)$ is the density of the finite nucleus.

The function $F(z)$ behaves like a Fermi function in the surface region, and it vanishes in the interior of the slab (see Ref. 9). The associated quantity $d\sigma^{(1)}/dz$ peaks outside half nuclear matter density.

We shall also calculate the response obtained in a local Fermi gas model (FGM), which we define as the weighted average of the density-dependent, infinite Fermi gas response using the weighting factor $|F(z)|^2$, i.e.,

$$\begin{aligned} S_{\text{FGM}}(q, \omega) &= -\int dz |F(z)|^2 \frac{1}{\pi} \\ &\quad \times \text{Im} \{ \Pi[\rho_{\text{FN}}(R+z), q, \omega] \}. \end{aligned} \quad (14)$$

Calculations with a similar local Fermi gas approximation have been performed previously.¹⁶

In the following section the surface response of the semi-infinite slab is compared to the infinite nuclear matter response. To make this comparison meaningful on an absolute scale we shall always display the surface response relative to the total single-scattering cross section [cf. Eq. (12)]

$$\sigma^{(1)} = \int dz |F(z)|^2 \rho_0(z). \quad (15)$$

This is in fact the sum rule for the direct response discussed in Ref. 12. The total response obtained from Eq. (10) may deviate from this sum due to Pauli blocking or the effect of residual interactions in the RPA response. For infinite nuclear matter one usually uses a plane wave as the external field [i.e., $F(z)=1$ in Eq. (11)]. The normalization that is equivalent to Eq. (15) is just the constant density ρ_0 , which in fact is the normalization used in Ref. 3.

III. NUMERICAL RESULTS

In this section we present the results of our numerical calculations of the isovector longitudinal and transverse spin response functions for the 500 MeV (p,p') reaction on ²⁰⁸Pb, at a scattering angle of 18.5 deg. The surface response of a semi-infinite slab of nuclear matter, Eq. (10), is calculated as described in the previous section and Ref. 12. We use exactly the same parameter set for the interactions [Eqs. (6) and (7)] that was used by Alberico *et al.*³ The external field that generates the surface response in our model (see Sec. II B) was determined from a total nucleon-nucleon cross section of $\sigma_{\text{NN}}=30$ mb. The associated single-scattering cross section on ²⁰⁸Pb becomes $\sigma^{(1)}=370$ mb, and we show the response functions relative to $\sigma^{(1)}$, as discussed previously.

The surface response depends on the orientation angle of the momentum transfer \mathbf{q} with respect to the slab surface. This dependence is rather weak and we show the average result in Fig. 2(a). The RPA responses are shown for excitation energies less than 100 MeV, and the longitudinal response is seen to be enhanced compared to the field-free response in this region, due to the dominant attractive pion exchange interaction. The rho-meson exchange interaction is weaker so the total interaction is repulsive in the transverse excitation channel, which leads to a reduction of the transverse response compared to the free response. The results, without including the delta-hole excitations (dashed curves), are also shown. Note that the polarization from the delta-hole excitation channels has a significant effect on the responses. The associated ratios of the longitudinal and transverse responses are shown in Fig. 2(b), both with and without (dashed curve) the delta-hole excitations. The enhancement of this ratio compared to 1 originates primarily from the pion and rho-meson exchange interactions.

In Ref. 12 the RPA responses for separable residual interactions were studied, and it was found that they yielded results quite close to those based on more realistic interactions. We have also calculated the longitudinal and transverse responses based on a separable representation of the

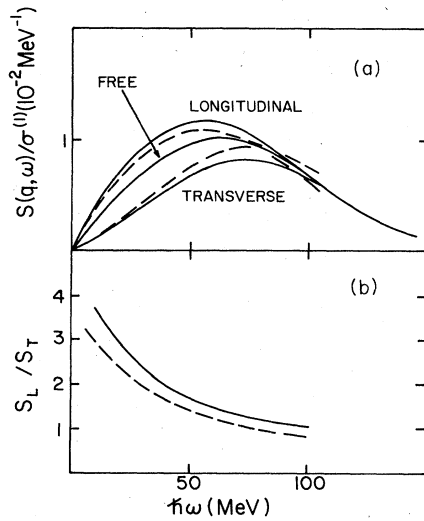


FIG. 2. The surface spin response functions in the longitudinal and in the transverse channels are shown in (a) together with the free response as functions of the excitation energy $\hbar\omega$ at the momentum transfer $q = 1.75 \text{ fm}^{-1}$. The solid curves include the effect of delta-hole excitations, whereas the dashed curves were obtained without this excitation channel. In (b) the associated ratios of the longitudinal and the transverse responses are shown, with (solid) and without (dashed) delta-hole excitations.

interactions given in Eqs. (6) and (7). We shall not give the detailed results here but only mention that the separable representation is unreliable for large momentum transfers perpendicular to the slab surface, since the induced density penetrates into the interior of the slab. It is, however, quite reasonable when the momentum transfer is along the surface in which case the induced density is lo-

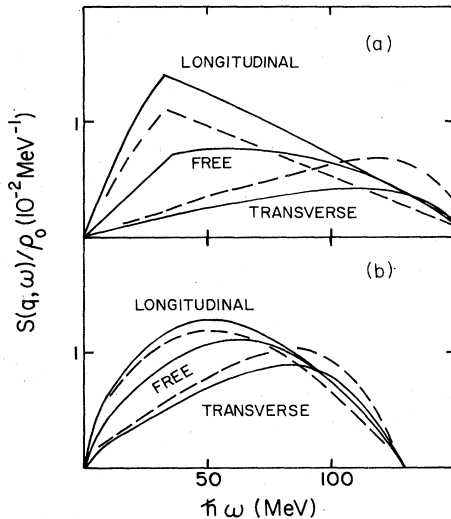


FIG. 3. Infinite matter spin responses as functions of the excitation energy at normal nuclear matter density (a) and at a density of one-third of nuclear matter density (b). The solid curves include the delta-hole excitations, while the dashed curves do not include these excitations. The momentum transfer is $q = 1.75 \text{ fm}^{-1}$.

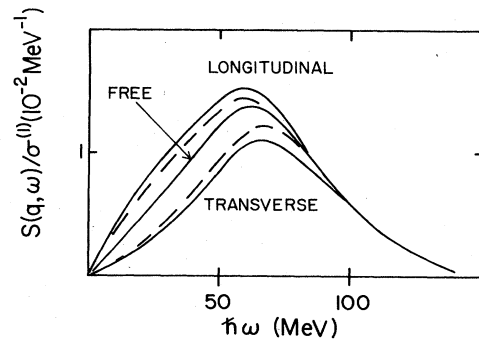


FIG. 4. Spin response functions in the local Fermi gas model are shown as functions of excitation energy, both with (solid) and without (dashed) the delta-hole excitation channel. The momentum transfer is $q = 1.75 \text{ fm}^{-1}$.

calized in the surface region.

For comparison we show the infinite nuclear matter responses in Fig. 3(a), both with and without (dashed curves) delta-hole excitations. The enhancement of the longitudinal response over the transverse response is very dramatic compared to the surface responses in Fig. 2. In order to demonstrate that this enhancement is very sensitive to the density we also show in Fig. 3(b) the infinite nuclear matter responses for a density of one-third of nuclear matter density.

The effect of the density dependence is incorporated in the simple, local Fermi gas model described in Sec. II B. The results are shown in Fig. 4. Although the actual magnitudes and shapes of these responses are somewhat different from the surface responses in Fig. 2, it turns out that the ratios of the longitudinal and the transverse response are quite similar. This is clearly seen in Fig. 5, where this ratio is shown for all three kinds of response calculations we have performed (SR: surface response; INM: infinite nuclear matter; and FGM: the local Fermi gas model) together with the values extracted from experiment.¹ Although the ratio is largely reduced compared to the infinite nuclear matter result, the ratio is about 2 in the surface response model at excitation energies of

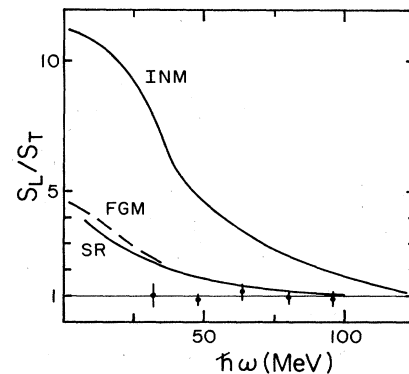


FIG. 5. The ratio of the longitudinal and the transverse spin response functions calculated in the surface response model (SR), the local Fermi gas model (FGM), and in infinite nuclear matter (INM) are compared with experimental data (Ref. 1).

30–40 MeV, whereas the experimental result is essentially 1.

We shall finally estimate the influence of the isoscalar spin response, which acts as a background on the isovector spin responses discussed previously. In Ref. 12 the double-differential cross sections for different excitation channels were factorized into an elastic nucleon-nucleon cross section times the associated response function. The measured ratio of the longitudinal and transverse spin responses of heavy nuclei (normalized to this ratio for deuterium as in the experiment) can thus be expressed in terms of the isospin-dependent spin responses S_L^τ and S_T^τ as follows:

$$S_L/S_T = \frac{P_L^{\tau=1} S_L^{\tau=1} + P_L^{\tau=0} S_L^{\tau=0}}{P_T^{\tau=1} S_T^{\tau=1} + P_T^{\tau=0} S_T^{\tau=0}}, \quad (16)$$

where the coefficients P_L^τ and P_T^τ are determined by the elastic nucleon-nucleon scattering amplitudes. For the specific analysis performed in Ref. 1 one finds that

$$P_L^\tau = |E_\tau|^2 / (|E_{\tau=0}|^2 + |E_{\tau=1}|^2), \quad (17)$$

$$P_T^\tau = |F_\tau|^2 / (|F_{\tau=0}|^2 + |F_{\tau=1}|^2),$$

where E_τ and F_τ are the isospin-dependent amplitudes constructed from the E and F amplitudes defined in Ref. 1. A recent phase-shift analysis of elastic nucleon-nucleon scattering by Arndt yields the values¹⁷ $|E_{\tau=1}/E_{\tau=0}|^2 = 3.6$ and $|F_{\tau=1}/F_{\tau=0}|^2 = 1.44$ for the kinematics studied in the experiment.

To evaluate the ratio in Eq. (16), we need an estimate of the isoscalar responses $S_L^{\tau=0}$ and $S_T^{\tau=0}$. The residual interactions in these channels are not very well known. The central part of the interaction is rather weak,¹³ and we shall use the free response to estimate $S^{\tau=0}$. We find that the ratio S_L/S_T is reduced from 2.3 to 1.7 for the lowest excitation energy considered, whereas the measured value is 1.01 ± 0.42 . There have been some suggestions that the $\tau=0$ tensor interaction is significant,¹⁸ which would reduce the predicted ratio further.

IV. CONCLUSION

We have calculated the isovector longitudinal and the transverse spin response induced by high-energy nucleon

scattering using the surface response model. We have demonstrated that the medium effects on the spin response functions are largely due to the nuclear surface. The ratio of the longitudinal and the transverse response functions is strongly reduced compared to infinite nuclear matter calculations. At $q = 1.75 \text{ fm}^{-1}$ this ratio comes out to be about 2 at excitation energies of 30 to 40 MeV, and it decreases with increasing excitation energy. As far as the ratio is concerned, the surface response calculation justifies the local Fermi gas model. Hence, there still remains a significant discrepancy between theory and experiment at lower excitation energies.

However, there are background effects which tend to decrease the difference between the longitudinal and the transverse responses induced by proton scattering. One is due to the isoscalar spin response, which cannot be eliminated in (p,p') reactions. Another effect comes from the spin-orbit interaction in the optical potential for the incoming nucleon, which flips by some amount the direction of the spin, and hence the distinction between a longitudinal and a transverse response is partly washed out. Both effects act as a background on the longitudinal and the transverse responses and reduce the ratio. Our estimate of the isoscalar background essentially resolves the discrepancy between theory and experiment; thus the inelastic scattering of 500 MeV protons is insensitive to the effects of meson exchange interactions. In this respect (p,n) reactions are more promising, since the isoscalar background is absent. An experiment is planned¹⁷ in the near future.

In contrast to the spin responses induced in high energy proton scattering, the EMC effect is a volume effect. Hence, the fact that the enhancement of longitudinal spin response in the proton induced reaction is weak or almost zero does not directly contradict the pionic interpretation of the EMC effect.

ACKNOWLEDGMENTS

We are grateful to Sam Austin, T. A. Carey, and J. B. McClelland for informative conversations. This work is supported by the National Science Foundation under Grant PHY-83-12245.

*Present address: Department of Physics, The University of Tennessee, Knoxville, TN 37996.

†Present address: Department of Physics, Tokyo Metropolitan University, Setagaya, Tokyo 158, Japan.

¹T. A. Carey *et al.*, Phys. Rev. Lett. **53**, 144 (1984).

²E. Oset, H. Toki, and W. Weise, Phys. Rep. **83**, 283 (1982).

³W. M. Alberico, M. Ericson, and A. Molinari, Nucl. Phys. **A379**, 429 (1982).

⁴C. H. Llewellyn-Smith, Phys. Lett. **128B**, 107 (1983).

⁵M. Ericson and A. W. Thomas, Phys. Lett. **124B**, 112 (1983).

⁶E. L. Berger, F. Coester, and R. B. Wiringa, Phys. Rev. D **29**, 298 (1984).

⁷D. Stump, G. F. Bertsch, and J. Pumplin, Michigan State University report, 1984.

⁸J. J. Aubert *et al.*, Phys. Lett. **123B**, 275 (1983).

⁹G. F. Bertsch and O. Scholten, Phys. Rev. C **25**, 804 (1982).

¹⁰R. J. Glauber and G. Matthiae, Nucl. Phys. **B21**, 135 (1970).

¹¹H. C. Chiang and J. Hüfner, Nucl. Phys. **A349**, 466 (1980).

¹²H. Esbensen and G. F. Bertsch, Ann. Phys. (N.Y.) **157**, 255 (1984).

¹³G. F. Bertsch, D. Cha, and H. Toki, Phys. Rev. C **24**, 533 (1981); H. Toki, D. Cha, and G. F. Bertsch, *ibid.* **28**, 1398 (1983).

¹⁴J. Speth *et al.*, Nucl. Phys. **A343**, 382 (1980).

¹⁵H. Toki and W. Weise, Phys. Lett. **92B**, 265 (1980).

¹⁶T. Izumoto, M. Ichimura, C. M. Ko, and P. J. Siemens, Phys. Lett. **112B**, 315 (1982).

¹⁷T. A. Carey and J. B. McClelland, private communication.

¹⁸S. Müller *et al.*, Phys. Lett. **120B**, 305 (1983); J. Wambach, A. D. Jackson, and J. Speth, Nucl. Phys. **A348**, 221 (1980).